Journal of Information Display, vol. 2, no. 3, 2001

Template-Based Carbon Nanotubes Field Emitter

Soo-Hwan Jeong, Ok-joo Lee, Sun-kyu Hwang, and Kun-Hong Lee*

Abstract

The growth of carbon nanotubes(CNTs) in anodic aluminum oxide(AAO) template and their application to a field emitter are described. AAO templates were fabricated by anodizing bulk aluminum and sputtered thin Al film on Nb-coated Si wafers. After Co catalyst had been electrochemically deposited into the bottom of the pores in AAO template, CNTs were grown by pyrolyzing C_2H_2. Depending on the reaction conditions, CNTs grew up to or over the top of the pores in AAO template with different structures. The morphology and structure of CNTs were observed with a scanning electron microscope and a transmission electron microscope. The diameter of CNTs strongly depended on the size of the pores in AAO template and the growing conditions. The electron field emission measurement of the samples resulted in the turn-on field of 1.9-2.2 V/μm and the field enhancement factor of 2450-5200. The observation of high field enhancement factors is explained in terms of low field screening effect.

Keywords : carbon nanotube, anodic alumina, field emitter, field screening

1. Introduction

Carbon nanotubes(CNTs) have drawn much attention because of their unique physical properties and their potential for a variety of applications[1,2]. One potential application is the field emitter tip[3,4]. Advantages of CNTs as a field emitter tip include small radius of the curvature, high aspect ratio, high chemical inertness and mechanical strength. Many researchers reported on densely packed CNTs on the electrode for this purpose. However, this approach has negative effect on the field enhancement due to the field screening effect [5]. Recently, Li *et al.*[6] reported the growth of aligned CNTs in the pores of an anodic aluminum oxide(AAO) using bulk aluminum. AAO can be prepared by anodizing Al in various electrolyte solutions with DC current. Varying anodizing conditions such as temperature, electrolyte, applied voltage, anodizing time and widening time, one can control density, the diameter and length of pores. Therefore, the diameter, length and density of CNTs may also be controlled by growing CNTs with AAO templates.

We used two types of Al samples. One is the bulk aluminum and the other is sputtered thin Al on Nb-coated Si wafer. After anodizing Al, Co catalyst was electrochemically deposited into the pore bottom of the AAO[6]. CNTs were grown in the pores of the AAO by catalytic thermal decomposition of acetylene. We report, in this paper, the growth of CNTs using AAO templates and its application to a field emitter tip.

2. Experimental

2. 1 Preparation of AAO templates

Two kinds of aluminum samples were used as the starting material. One is the pure aluminum sheet of 1 mm in thickness (hereafter, ALS) and the other is the sputtered Al film of 300 nm in thickness on Nb-coated Si wafer (hereafter, ALF). ALS was degreased in acetone solution by ultrasonication and then electropolished in

Manuscript received August 19, 2001; accepted for publication April 20, 2001.
This work was supported by LG Electronics Inc. and the Ministry of Education of Korea.
* Member, KIDS.
Corresponding Author : Kun-Hong Lee
Department of Chemical Engineering, Pohang University of Science and Technology, san 31, Hyoja-dong, Nam-gu, Kyungbuk 790-784, Korea.
E-mail : cc20047@postech.ac.kr **Tel** : +54 279-2271 **Fax** : +54 279-8298

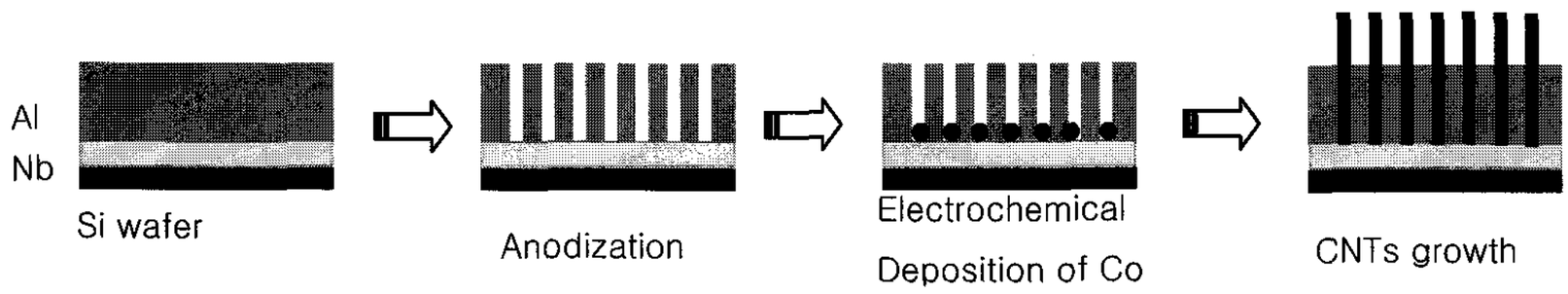

Fig. 1. Schematic of the fabrication process of CNTs field emitter (ALF).

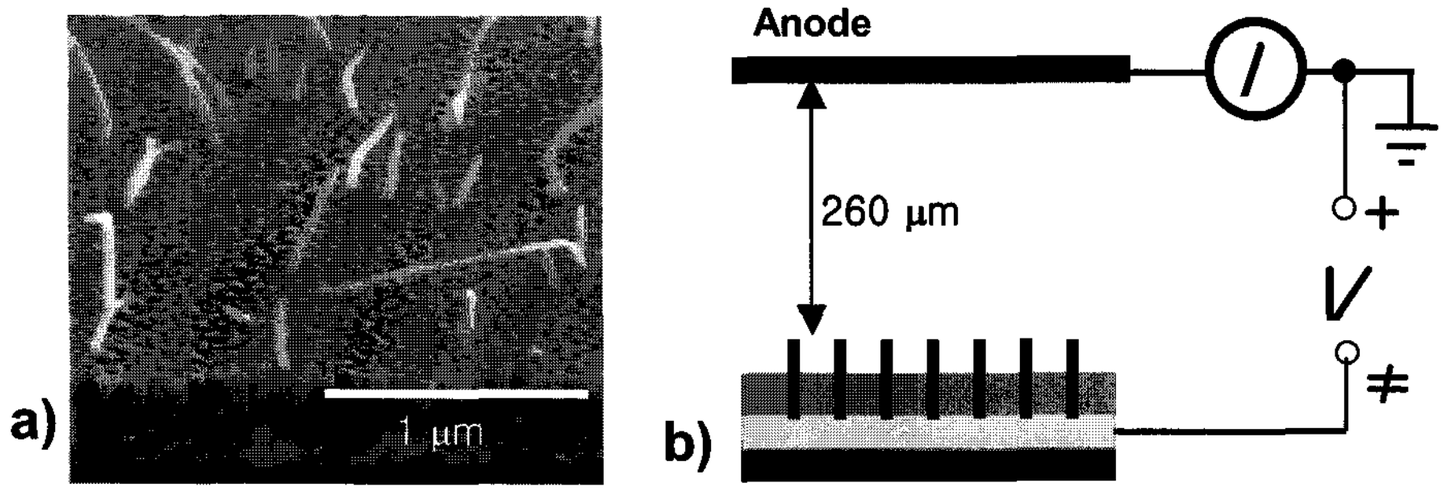

Fig. 2. a) SEM micrograph of a template based CNTs; b) Schematic of a field emission measurement set up (Anode : P-22 CRT phosphor/ITO /glass, Spacer : 260 μm thick).

the mixture of perchloric acid/ethanol solution to obtain the mirror finish. ALF containsed 2 atomic % of Nd to achieve a smooth surface. ALF was anodized without degreasing and electropolishing. Both types of samples were anodized in 0.3M oxalic acid solutions at 15 °C, using Pt sheet as the cathode. Anodizing voltage was 40V. Two step anodization was carried out to obtain the ordered pore array for the ALS. After the first anodizing step, AAO on the ALS was removed using the mixture of chromic acid and phosphoric acid, followed by the second anodization.

Samples were rinsed with deionized water after anodization. To facilitate the electrochemical deposition of Co particle by thinning the barrier layer, AAO template were dipped into the 0.1M phosphoric acid at 30 °C for 20~50 minutes. Cobalt particles were electrochemically deposited in the pores of the AAO template at 3V~16V ac using cobalt sulfate electrolyte stabilized with boric acid at room temperature.

The microstructure of AAO templates was observed with the field emission scanning electron microscope (FESEM, Hitachi S-4200).

2. 2 Growth of cnts with AAO templates

Co particles were reduced in the gas mixture of 2% H_2 and 98 % Ar at 600 °C for 1hr. The CNTs were then grown by catalytic pyrolysis of C_2H_2 in Ar carrier gas for 5 minutes~2 hours at 650 °C in a tube reactor. The concentration of C_2H_2 and H_2 were varied. The morphology and structure of CNTs were observed with the field emission scanning electron microscope(FESEM, Hitachi S-4200) and the high resolution transmission electron microscope(HRTEM, Philips CM20). An illustration of the fabrication process in this work is shown in Fig.1. For the ALS, remaining Al layer after anodization served as an electrode for the electrochemical deposition of Co.

2.3 Field emission measurement

In case of the ALS, the remaining Al after anodization served as the cathode for the field emission measurement, while Nb layer beneath the thin sputtered Al film was used as the cathode for ALF. The glass plate pre-coated with P22 phosphor and ITO layer was used as the anode. The samples were separated from the anode by a 260 μm thick spacer. Field emission measurements were carried out in a vacuum chamber at about 2×10^{-7} Torr. The Keithley 237 source-measure unit was used to apply voltage and to measure the emitting current (with pA sensitivity and up to 1mA). The images on the P22 phosphor/ITO/glass were captured with digital camera. Typical template-based CNTs field emitter and emission measurements set-up are shown in Fig. 2.

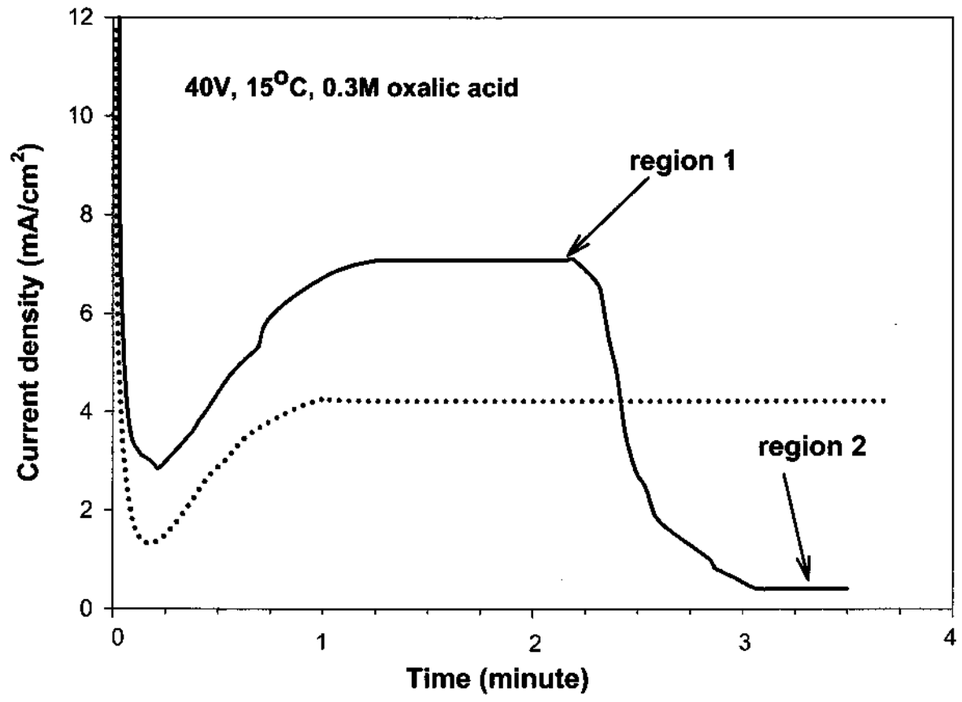

Fig. 3. Current density vs time curve of Al during AAO formation (— ALF and ···ALS)

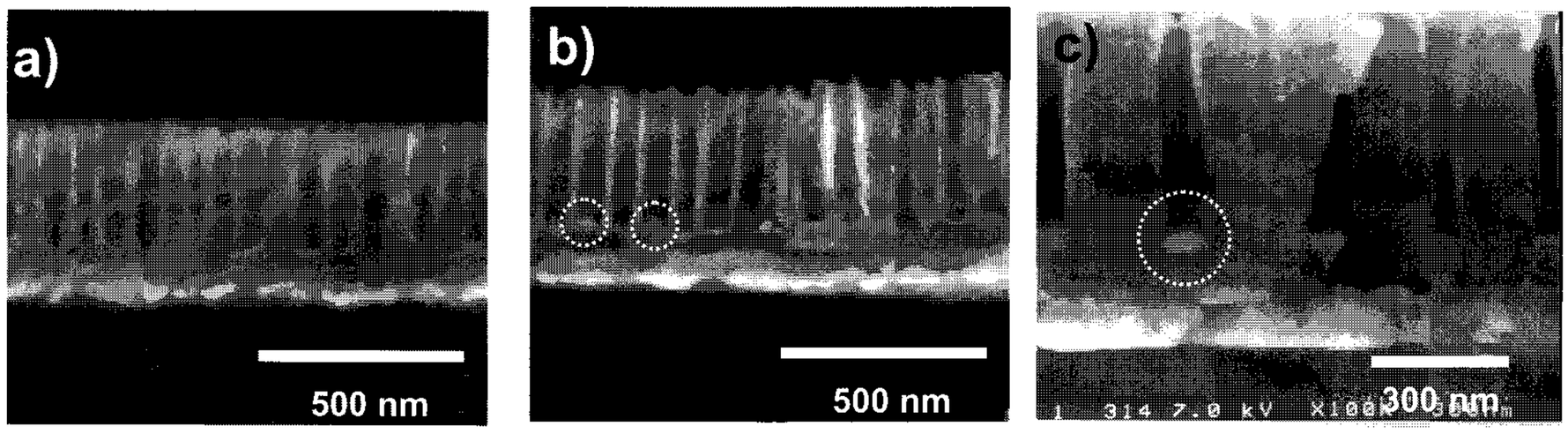

Fig. 4. SEM images of AAO templates. a) cross sectional view of the pore array at region 1 (50 min pore widening in 0.1M phosphoric acid soln. at 30 °C) b) cross sectional view of the pore array at region 2 (50 min pore widening in 0.1M phosphoric acid soln. at 30 °C) c) cross sectional view of the pore array at region 2 at 120V in 10wt.% phosphoric acid.

3. Results and Discussions

3.1 AAO templates

Fig.3 shows the current density vs. time curve of two aluminum samples at a cell voltage of 40V in 0.3M oxalic acid at 15 °C. For the ALF, anodizing current density was about 7mA/cm^2 during anodization of the Al layer (to the region 1), then abruptly decreased to 0.2 mA/cm^2 with color change but not to zero (region 2). Anodizing current density of ALF was 1.7 times larger than that of ALS resulting in 1.7 times faster anodizing rate.

It is thought that the current at the region 2 corresponds to the current which is triggered by the Nb_2O_5 pillar formation at the bottom of AAO template. In fact, Vorobyova *et al.*[7] reported that the Ta_2O_5 pillar formation at AAO pore bottom after the anodization of Al film on Ta substrate. Iwasaki *et al.*[8] also showed that the Nb_2O_5 channel formation at the barrier layer in Al/Nb system during anodization. Figs. 4.-b) and c) show the Nb_2O_5 pillar formed at region 2. When anodization was stopped immediately before observing a current decrease (arrow for region 1 in Fig. 3), pillar formation at the pore bottom of AAO template was not detected (see Fig.4-a). This pillar formation was enhanced when higher anodizing voltage was applied as shown in Fig. 4.-c). On the other hand, when Cr was used as an electrode under Al, current increased after Al was completely anodized and the alumina layer was separated from the electrode.

The pore diameter was about 13 nm after anodization of the ALF. It was enlarged to approximately 60nm after widening in 0.1M phosphoric acid at 30 °C for 50 minutes.

Co catalyst was electrochemically deposited at the pore bottom of AAO template in the 5 % $CoSO_4 \cdot 7H_2O$ solution stabilized with 2 % H_3BO_3 by applying AC voltage. After thinning the barrier layer for 50 min in

widening solutions, 15 Vrms AC was applied for the ALS. Ca. 1 min was required to fill the pore bottom with Co particles having the aspect ratio of 1. Surprisingly, Co was deposited at only 3 Vrms AC in AAO template of ALF. Moreover, it took only 10 seconds to obtain the Co particles of aspect ratio of 1. Fig. 5.-a) and Fig. 5.-b) show the Co deposited in the AAO template depicted in Fig. 4.-a) and Fig. 4.-b) at 3Vrms for 10 seconds. Although the exact role of Nd is not clear, it is certain that Nd plays a crucial role in lowering the AC voltage of electrochemical deposition. Herrera-Erazo *et al.*[9] reported that the field strength for film growth and the thickness of barrier-type oxide reduced for the Nd-containing Al than for the pure Al. Thinner oxide layer partially explains the low AC voltage for electrochemical deposition.

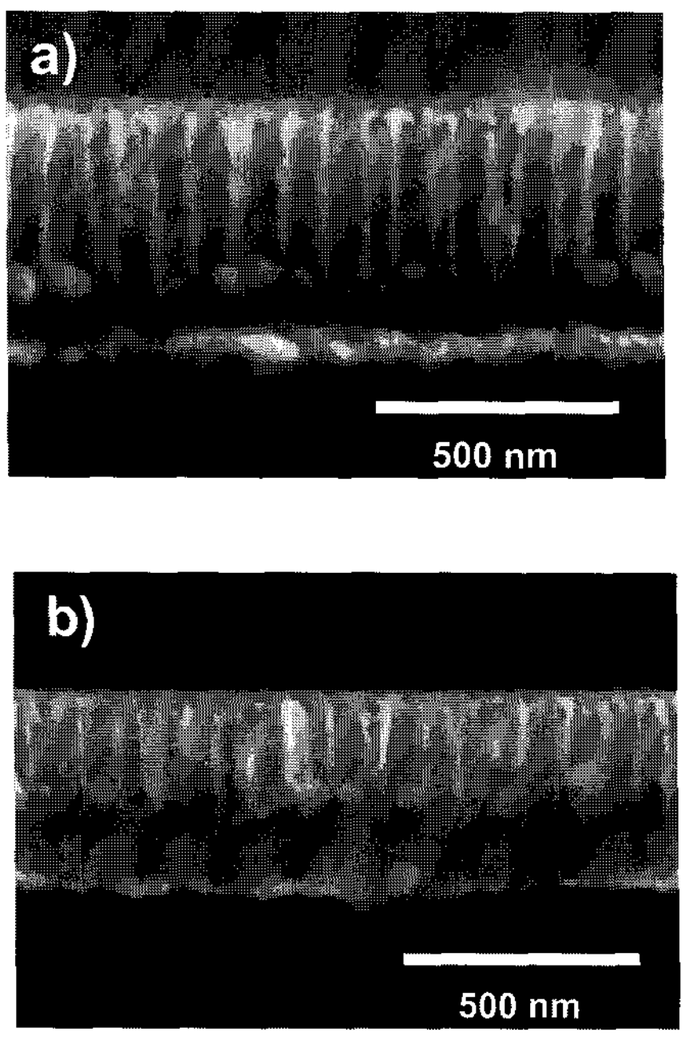

Fig. 5. SEM image of AAO template embedded with Co particles. a) cross sectional view of AAO template formed at region 1 b) cross sectional view of AAO template formed at region 2.

3.2 Template based CNTs

The CNTs were synthesized with Co-containing AAO templates in the mixture of 10 % acetylene and 90 % argon at 650 °C for 2h. The surface of the AAO template was covered by a thin carbon film. This surface carbon deposition was removed by O_2 plasma treatment (RF power=100W, O_2 flow rate=20sccm, Vbias=-200V, time=5min). Samples were then immersed in HF solution for a few seconds to expose CNTs tips shown in Fig. 6. When CNTs were grown at lower acetylene concentration (2 % C_2H_2 in Ar), some overgrown CNTs with diameters smaller than pore diameter were observed. Surface carbon deposition was thinner than those formed with high acetylene concentration.

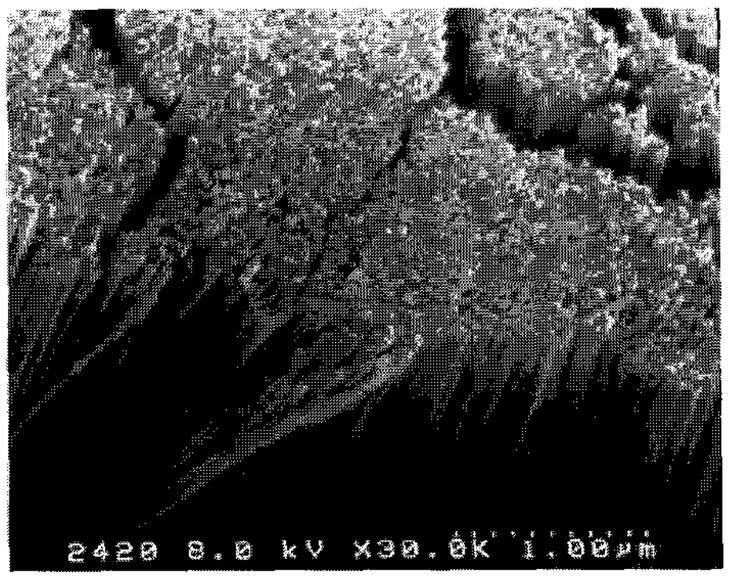

Fig. 6. SEM image of CNTs grown at 650 °C under 10 %C_2H_2/90 %Ar after O_2 plasma treatment.

Another major factor on CNTs morphology was hydrogen concentration in the gas mixture. Hydrogen has been thought to be a catalyst for carbon-producing reactions[10]; or it might serve to keep the exposed catalyst surface "clean" from encapsulating carbon that would deactivate it[11]. In our study, the addition of H_2 in the gas mixture changed CNTs morphology to a great extent. When gas composition was changed to 20 % H_2, 10 % C_2H_2 and 70 % Ar, CNTs were not confined inside the pore and overgrown out of the pore with almost the same diameter as that of pore and length of about one to several tens of micrometers depending upon reaction time (see Fig. 7-a). However, CNTs were not overgrown from all pores embedded with Co catalyst. In this case, Co particles were found to be at the middle or tip of CNTs as shown in Fig. 7-b). This is a totally different result from the case in which no hydrogen was added. This is attributed to the "cleaning effect" of hydrogen, which prevents Co catalyst from deactivation by carbon deposition on the active site of catalyst particles.

Further investigation by TEM analysis gives deeper insight to the effect of gas composition on CNTs synthesis by acetylene decomposition. Fig.8-a). shows the TEM image of CNTs synthesized in the template without hydrogen, which form a highly aligned ensemble with the same length as the template. From the HRTEM

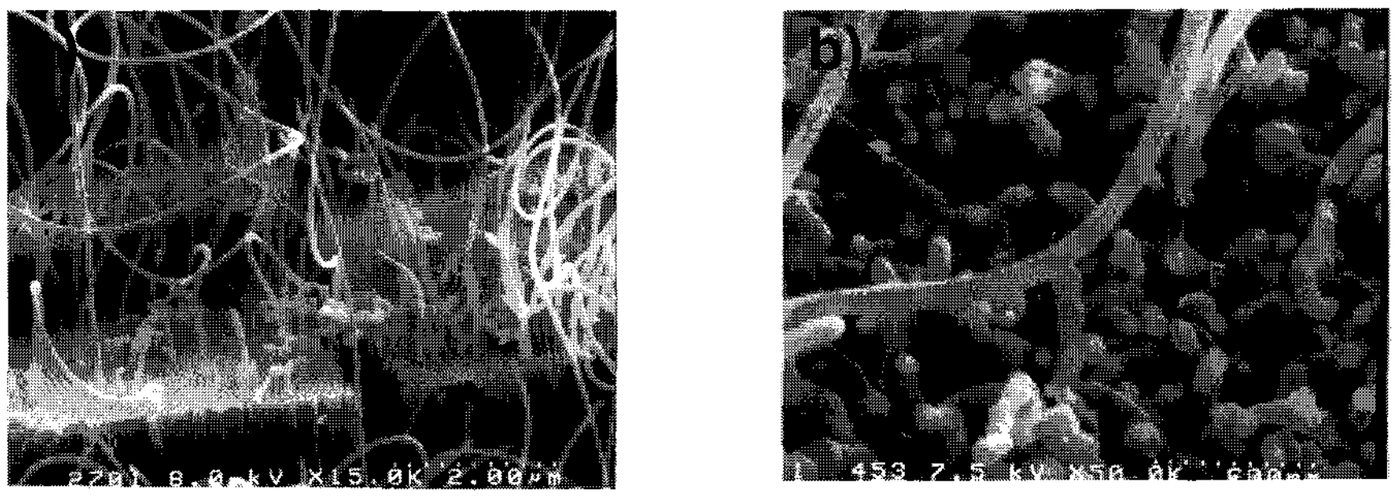

Fig. 7. (a) SEM image of CNTs grown at 650 °C under 20 %H_2/10 %C_2H_2/70 %Ar (b) Same sample with higher magnification.

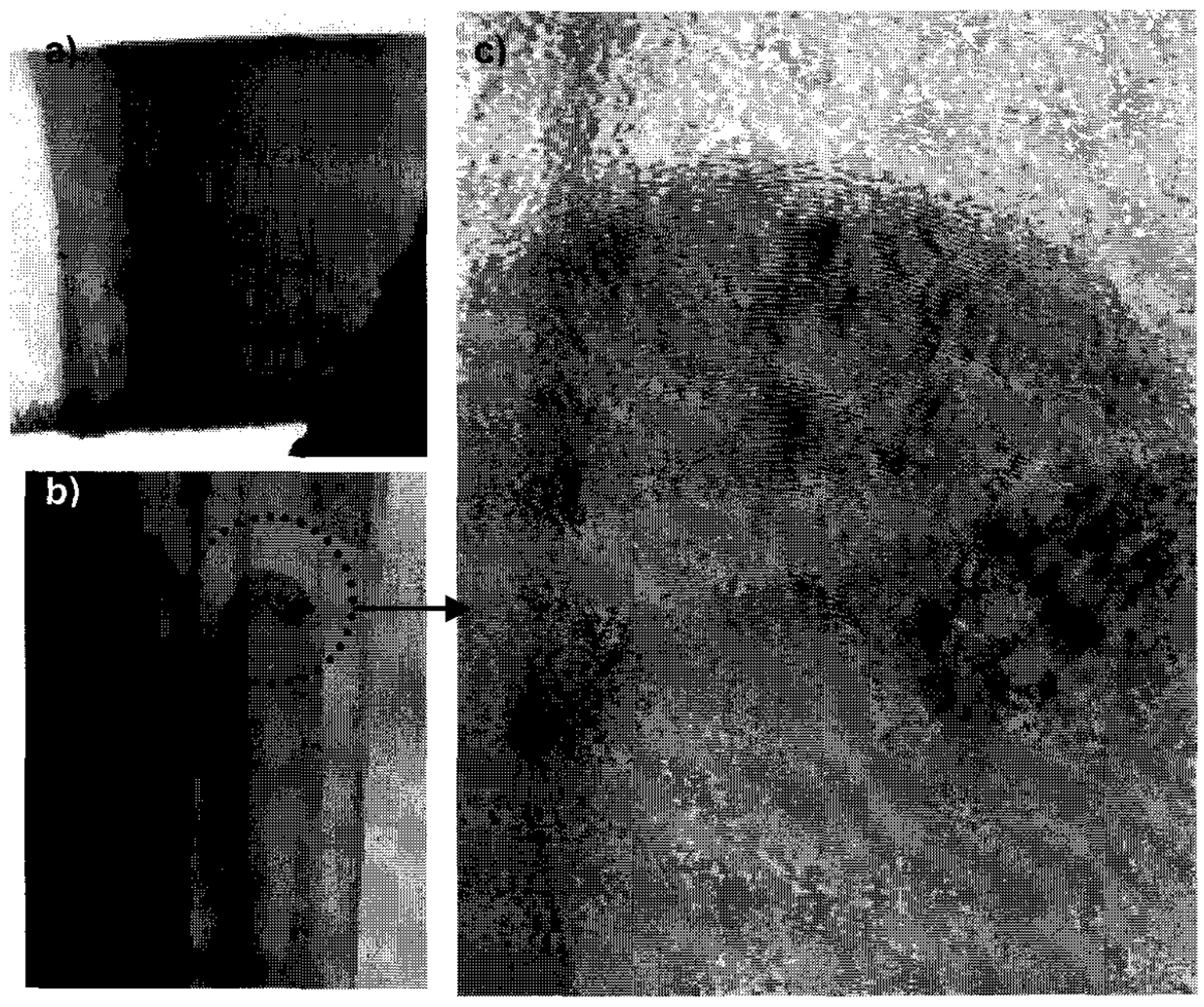

Fig. 8. TEM image of the CNTs grown at 650 °C under 10 %C_2H_2/90 %Ar.

image of CNTs, we could identify them as an agglomeration of amorphous carbon. On the other hand, at the bottom part of these CNTs, well-graphitized multi-walled CNTs were observed. These CNTs were of short length less than 1 μm and had closed ends. Fig.8-b) depicts TEM image of bottom part and Fig.8-c) is the HRTEM image of the areas circled in Fig.8-b which shows closed multi-walled CNTs.

The CNTs with closed-ends and hollow cores were observed with the mixed gas containing hydrogen. As shown in Fig. 9, the outermost layers consist of graphite layers aligned parallel to tube axis (i.e. typical multi-walled CNTs). In fact, the CNTs growth in AAO template is believed to be a complex process which involves competitive hydrocarbon decomposition by both cobalt particles at the bottom of the pores and the AAO template itself. In our case, it has been proven that although cobalt is much more active catalyst for acetylene decomposition, alumina can also exhibit catalytic activity under certain conditions. When the concentration of acetylene in feed gas is high, the deactivation of Co catalyst is fast and the catalytic role of alumina becomes dominant. Therefore, CNTs were not overgrown from the pores because the amorphous carbon deposited on the wall of pores in AAO template blocks the growth of CNTs on Co particles at the bottom of pores.

3.3 Field emission from CNTs

Three samples were chosen to investigate the effect of CNTs on the field emission. Fig. 10 shows the

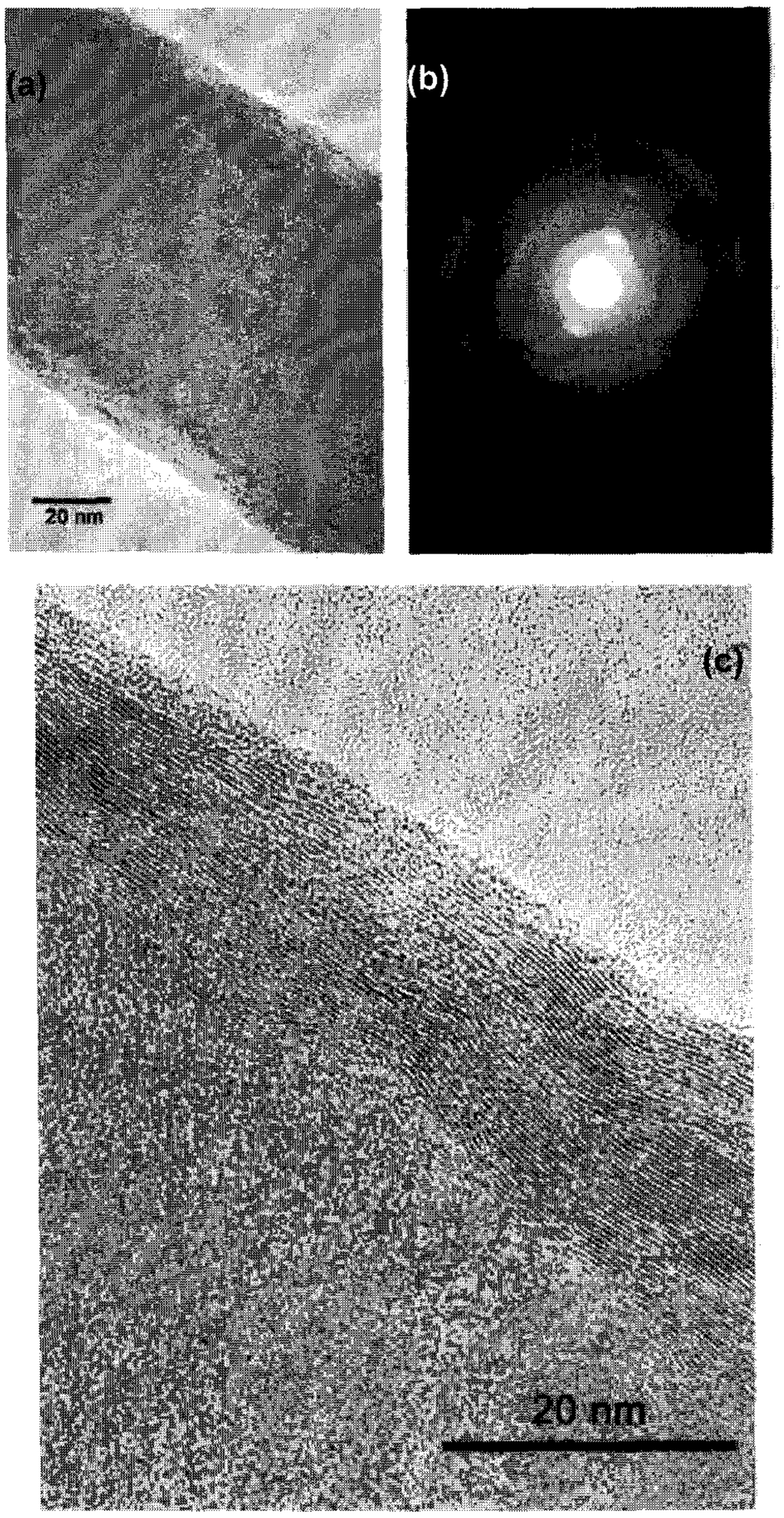

Fig. 9. TEM image and electron diffraction pattern of the CNTs grown at 650 °C under 10 %C_2H_2/20 % H_2/70 %Ar. (a) Low magnification TEM image, (b) Electron diffraction pattern, (c) High magnification TEM image.

surfaces of the AAO samples after CNTs growth. The conditions for the preparation of samples are given in Table 1.

I-V relationships after 4~5 subsequent I-V cycles were plotted in Fig.11. The E_{to} (turn-on field) needed to produce an emission current density of 10 μA/cm^2 was obtained from the I-V curve. For these samples, E_{to} were found to be in the range of 1.9-2.2 V/μm. This is similar to the previously reported values. [12,13,14] Fig.12 shows the Fowler-Nordheim plots of our samples. The emission data are generally in agreement with the Fowler-Nordheim equation, confirming that the current was indeed caused by electron field emission. We have also estimated the field enhancement factor β. From these plots, one can obtain the slope that depends on ϕ, d, and β. The slope of the F-N plot is equal to $B\phi^{3/2}\, d/\beta$, where the constant $B = 6.87\times 10^9 \mathrm{VeV}^{-3/2}\ \mathrm{m}^{-1}$[14]. d is the distance between CNTs and anode. The work function ϕ of CNTs was assumed to be that of graphite (=5eV). The field enhancement factor β was then estimated using the above equation. The field enhancement factors of samples A, B and C obtained from the F-N plots (Fig. 12.) were 2450, 5200 and 3360, respectively.

The main difference among the samples A, B and C

Table 1. Samples used to measure the field emission current.

	Start material	Anodizing	Pore widening	Co deposition	Growing conditions (Total flow rate = 200 sccm)
Sample A	ALS	Two step 0.3M oxalic acid, 15°C, 40V, 10 min 2nd anodizing	50 min	1min 16Vrms	2% C_2H_2, 10% H_2 with Ar 10 min, 650°C
Sample B	ALS	Two step 0.3M oxalic acid, 15°C, 40V 10 min 2nd anodizing	50 min	1min 16Vrms	10% C_2H_2, 20% H_2 with Ar 15 min, 650°C
Sample C	ALF	One step 0.3M oxalic acid, 15°C, 40V	50 min	10 sec 3Vrms	10% C_2H_2, 20% H_2 with Ar 15 min, 650°C

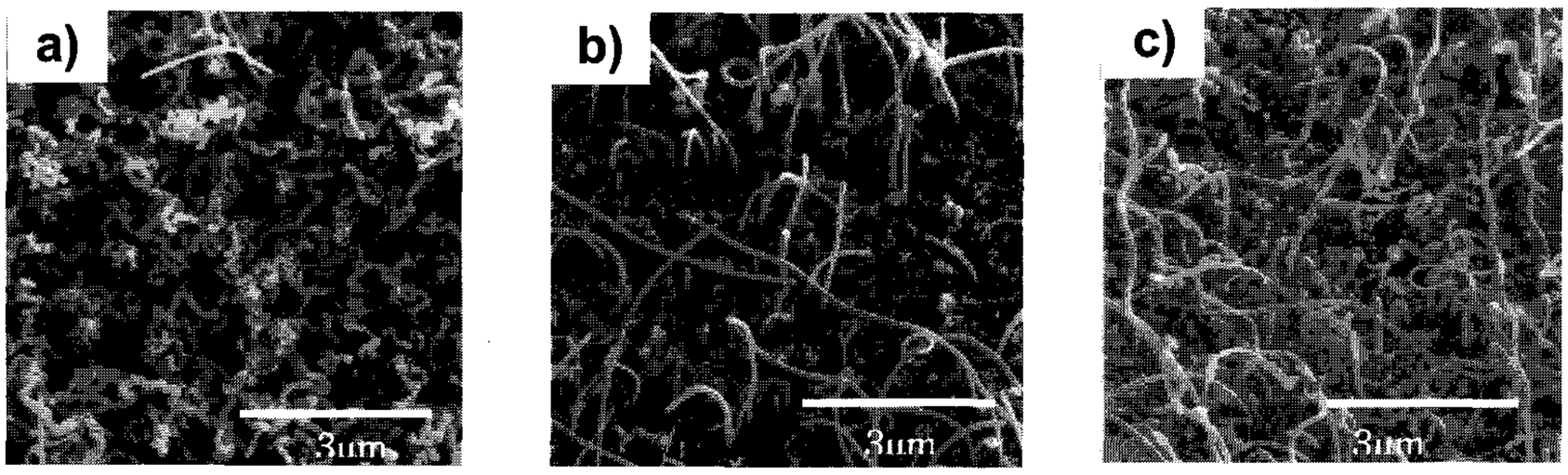

Fig. 10. SEM image of CNTs field emitter ; a) sample A, b) sample B, and c) sample C.

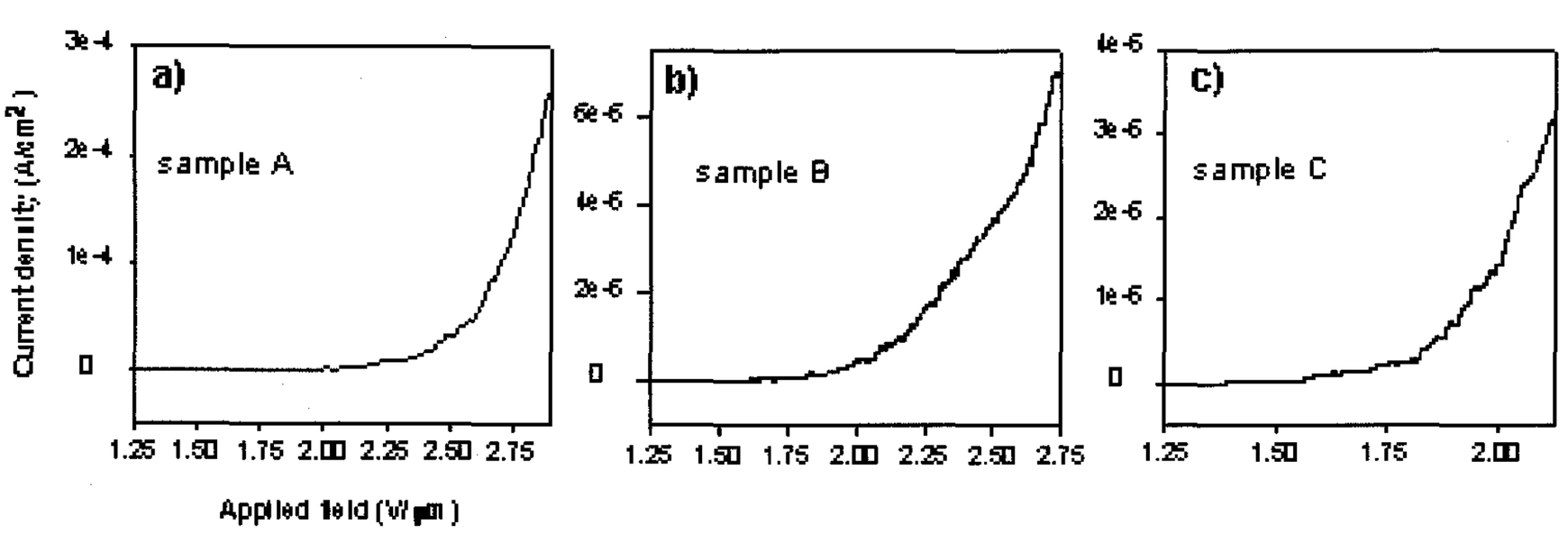

Fig. 11. Emission current density – Applied field curves for the template-based CNTs.

from the SEM images in Fig. 10 was the density of overgrown CNTs. Density of CNTs in the sample A is the highest resulting in the lowest β value. Sample B which had the lowest density of CNTs showed the highest β value, as expected. These β values were relatively higher than those of other researchers [14,15]. Their β values of multi-walled CNTs were in the range of 800~1900. The CNTs density of other researchers were in the range of 10^9 ~10^{12} tips/cm^2.

L.Nilsson and co-workers[5] predicted that an inter-tube distance of about 2 times the height of the CNTs were required to avoid field screening effect. The CNTs of 1 μm height corresponded to the density of 2.5×10^7 tips/cm^2 . The density of sample B was about 10^8 tips/cm^2 and the length of CNTs was shorter than that of other samples. The straightness was relatively good. Therefore, it is thought that sample B had a large value of β. The field emission measurements of other samples grown at various conditions are in progress.

4. Conclusions

We have successfully fabricated template-based CNTs as a field emitter. The morphology and structure of CNTs were strongly affected by the AAO template, itself,

as well as the growing conditions. When hydrogen was absent in feed gas, the CNTs were not overgrown out of the pores in the AAO template under our conditions. The bottom part of CNTs was multi-walled CNTs and the upper part was amorphous carbon deposit. CNTs were overgrown in the presence of hydrogen. Overgrown CNTs have graphite layers aligned parallel to tube axis with hollow core.

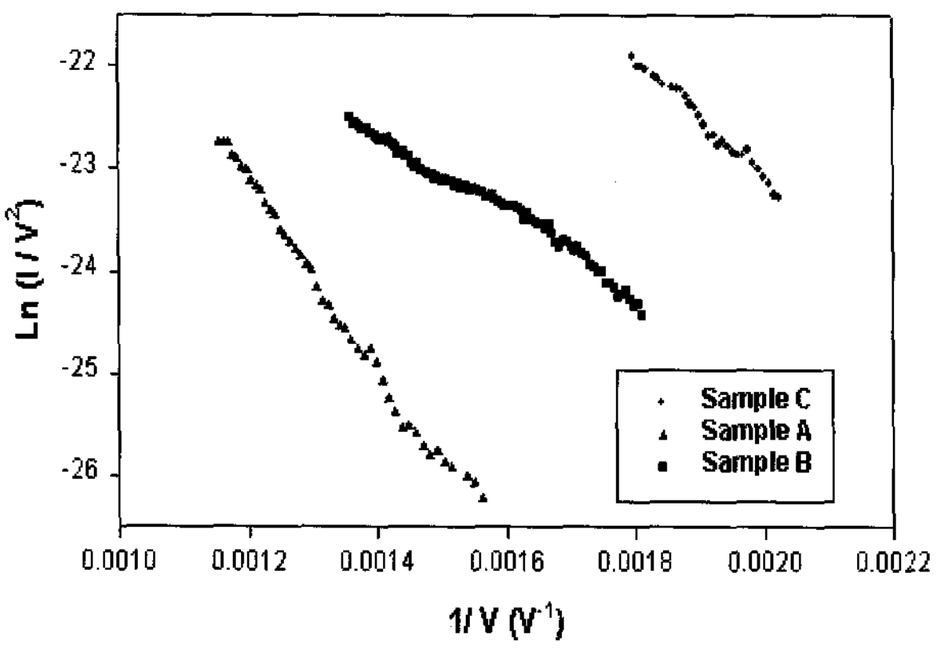

Fig. 12. Fowler-Nordheim plots of field emission for the template-based CNTs emitters.

We observed significant values of field enhancement factor of 2450-5200. To avoid the field screening effect, low density of CNTs was favored. The high values of field enhancement factor resulted from the low density of CNTs in our samples. Systematic investigation of field emission from other samples grown under various conditions is in progress.

Acknowledgement

The authors would like to thank LG Electronics Inc. and the Ministry of Education of Korea for its financial support toward the Electrical and Computer Engineering Division at POSTECH through its BK21 program.

References

[1] W. A. De Heer, A. Chatelain and D. Ugarte, "A carbon nanotube field-emission electron source," Science, vol. 270, pp. 1179-1180, 1995.

[2] P. G. Collins, A. Zettle, H. Bando, A. Thess and R. E. Smally, "Nanotube nanodevice," Science, vol. 278, pp. 100-102, 1997.

[3] Y. Saito and S. Uemura, "Field emission from carbonnanotubes and its application to electron sources," Carbon, vol. 38, pp. 169-182, 2000.

[4] J. M. Bonard, T. Stockli, F. Maier, W. A. De Heer, A.Chatelain, D. Ugarte, J. P. Salvetat and L. Forro, "Field-emission-induced luminescence from carbon nanotubes," Phys. Rev. Lett., vol. 81, pp. 1441-1444, 1998.

[5] L. Nilsson, O. Groening, C. Emmenegger, O. Kuettel, E. Schaller, L. Schlapbach, H. Kind, J. M. Bonard and K. Kern, "Scanning field emission from patterned carbon nanotube films," Appl. Phys. Lett., vol. 76, pp. 2071-2073, 2000.

[6] J. Li, C. Papadopoulos, J. M. Xu and M. Moskovits, "Highly-ordered carbon nanotube arrays for electronic applications," Appl. Phys. Lett., vol. 75, pp. 367-369, 1999.

[7] A. I. Vorobyova and E. A. Outkina, "Study of pillar microstructure formation with anodic oxides," Thin Solid Films, vol. 324, pp. 1-10, 1998.

[8] T. Iwasaki, T. Motoi and T. Den, "Multiwalled carbon nanotubes growth in anodic alumina nanoholes," Appl. Phys. Lett., vol. 75, pp. 2044-2046, 1999.

[9] A. E. Herrera-Erazo, H. Habazaki, K. Shimizu, P. Skeldon and G. E. Thompson, "Anodic film growth on Al-Nd alloys," Corros. Sci., vol. 42, pp. 1823-1830, 2000.

[10] R. G. Olsson and E. T. Turkdogan, " Catalytic effect of iron on decomposition of carbon monoxide," Met. Trans., vol. 5, pp. 21-26, 1974.

[11] A. I. La Cava, C. A. Bernardo and D.L. Trimm, "Studies of deactivation of metals by carbon deposition," Carbon, vol. 20, pp. 219-223, 1982.

[12] Q. H. Wang, T. D. Corrigan, J. Y. Dai, R. P. H. Chang and A.R. Krauss, "Field emission from nanotube bundle emitters at low fields,"Appl. Phys. Lett., vol. 70, pp. 3308-3310, 1997.

[13] S. Fan, M. G. Chapline, N. R. Franklin, T. W. Tombler, A. M. Cassell and H. Dai, "Self-oriented regular arrays of carbon nanotubes and their field emission properties," Science, vol. 283, pp. 512-514, 1999.

[14] J. M. Bonard, J. P. Salvetat, T. Stockli, L.Forro and A. Chatelain, "Field emission from carbon nanotubes : perspectives for applications and clues to the emission mechanism," Appl. Phys. A, vol. 69, pp. 245-254, 1999.

[15] D. N. Davydov, P. A. Sattari, D. AlMawlawi, A. Osika, T. L. Haslett and M. Moskovits, "Field emitters based on porous aluminum oxide template," J. Appl. Phys., vol. 86, pp. 3983-3987, 1999.